# Sesquiterpenoids From the Antarctic Fungus *Pseudogymnoascus* sp. HSX2#-11

Ting Shi[1], Xiang-Qian Li[1,2], Li Zheng[3,4], Ya-Hui Zhang[5,6], Jia-Jia Dai[1], Er-Lei Shang[7], Yan-Yan Yu[1], Yi-Ting Zhang[1], Wen-Peng Hu[1] and Da-Yong Shi[1,2]*

[1] State Key Laboratory of Microbial Technology, Institute of Microbial Technology, Shandong University, Qingdao, China, [2] Laboratory for Marine Drugs and Bioproducts of Qingdao National Laboratory for Marine Science and Technology, Qingdao, China, [3] Key Laboratory of Marine Eco-Environmental Science and Technology, First Institute of Oceanography, Ministry of Natural Resources, Qingdao, China, [4] Laboratory for Marine Ecology and Environmental Science, Qingdao Pilot National Laboratory for Marine Science and Technology, Qingdao, China, [5] Key Laboratory of Marine Drugs, The Ministry of Education of China, School of Medicine and Pharmacy, Ocean University of China, Qingdao, China, [6] Laboratory for Marine Drugs and Bioproducts, Qingdao National Laboratory for Marine Science and Technology, Qingdao, China, [7] State Key Laboratory of Pharmaceutical Biotechnology, School of Life Sciences, Nanjing University, Nanjing, China

The fungal strains *Pseudogymnoascus* are a kind of psychrophilic pathogenic fungi that are ubiquitously distributed in Antarctica, while the studies of their secondary metabolites are infrequent. Systematic research of the metabolites of the fungus *Pseudogymnoascus* sp. HSX2#-11 led to the isolation of six new tremulane sesquiterpenoids pseudotremulanes A–F (**1**–**6**), combined with one known analog 11,12-epoxy-12$\beta$-hydroxy-1-tremulen-5-one (**7**), and five known steroids (**8**–**12**). The absolute configurations of the new compounds (**1**–**6**) were elucidated by their ECD spectra and ECD calculations. Compounds **1**–**7** were proved to be isomeride structures with the same chemical formula. Compounds **1/2**, **3/4**, **1/4**, and **2/3** were identified as four pairs of epimerides at the locations of C-3, C-3, C-9, and C-9, respectively. Compounds **8** and **9** exhibited cytotoxic activities against human breast cancer (MDA-MB-231), colorectal cancer (HCT116), and hepatoma (HepG2) cell lines. Compounds **9** and **10** also showed antibacterial activities against marine fouling bacteria *Aeromonas salmonicida*. This is the first time to find terpenoids and steroids in the fungal genus *Pseudogymnoascus*.

Keywords: Antarctic fungus, *Pseudogymnoascus* sp. HSX2#-11, sesquiterpenoids, steroids, cytotoxicity, antibacterial activity

## INTRODUCTION

Tremulanes, a family of sesquiterpenoids with characteristic structures of 5/7 fused bicyclic system, were rarely discovered in nature until 2015 (Guo et al., 2016). However, from 2016 to 2020, about 60 tremulane derivatives were found (Guo et al., 2016; Isaka et al., 2016; Wu, 2016; Chen et al., 2017, 2018; Cong et al., 2020; Wang et al., 2017, 2020; Ding et al., 2018, 2019, 2020a,b; Zhou et al., 2018; Duan et al., 2019; Wu et al., 2019, 2020; He et al., 2020; Lee et al., 2020; Shi et al., 2020; Sun C.-T. et al., 2020), and the number is twice as many as before. Most of them were isolated from the cultures of the basidiomycetes *Irpex lacteus* (Chen et al., 2018, 2020; Ding et al., 2018, 2019, 2020a,b;

Zhou et al., 2018; Duan et al., 2019; Wu et al., 2019; Shi et al., 2020; Sun C.-T. et al., 2020; Wang et al., 2020). All the tremulanes isolated from 2016 to 2020 were derived from fungi, except one derivative, which was obtained from a traditional Chinese medicine tabasheer (Wu, 2016). Some of them were discovered to have different bioactivities, such as tremutin A with the inhibition of the lipopolysaccharide-induced proliferation of B lymphocyte cells (Wang et al., 2020), and 5-demethyl conocenol C showed antifungal activities (Wu et al., 2019).

The extreme environments of Antarctica, including cold, dry climate and intense solar radiations, have nurtured a number of unique microbial resources (Cong et al., 2020). It has been proved that Antarctic microorganisms, especially fungi, have the potential capacity to produce novel secondary metabolites to adapt to the harsh environments (Kwon et al., 2017; Rusman et al., 2018; Yu et al., 2019; Sun C. et al., 2020). *Pseudogymnoascus* are known as a kind of psychrophilic pathogenic fungi with ubiquitous distribution in Antarctica (Rosa et al., 2020; Santos et al., 2020; Martorell et al., 2021). These fungal strains have been proved to have the abilities to produce cold-adapted enzymes to adapt severe cold Antarctic environment (Loperena et al., 2012; Poveda et al., 2018). *Pseudogymnoascus* can be antagonistic fungi against potato scab pathogens from potato field soils (Tagawa et al., 2010) and have been certified to be one of the predominant microbial colonizers in the root endosphere and rhizosphere of turfgrass systems (Xia et al., 2021). The extracts of some of *Pseudogymnoascus* strains exhibit potent bioactivities, such as antimicrobial, herbicidal, and antitumoral activities (Henríquez et al., 2014; Gonçalves et al., 2015; Gomes et al., 2018; Ferrarezi et al., 2019). However, only four studies have been done on the secondary metabolites of the genus *Pseudogymnoascus* until now, as far as we know, and most of the obtained structures focus on polyketides, showing antimicrobial activities (Figueroa et al., 2015; Guo et al., 2019; Fujita et al., 2021; Shi et al., 2021). Rare studies about the secondary metabolites of these fungi enlighten that there is latent space for searching novel compounds. *Pseudogymnoascus* sp. HSX2#-11 was an Antarctic fungus isolated from a soil sample of the Fields Peninsula, which can produce abundant and various secondary metabolites, according to our previous research on the fingerprint spectrum and molecular network of its ethyl acetate extract of the fermentation broth (Shi et al., 2021). Further chemical investigation resulted in the isolation and identification of six new tremulane sesquiterpenoids, pseudotremulanes A–F (1–6), together with one known analog 11,12-epoxy-12$\beta$-hydroxy-1-tremulen-5-one (7; Zhou et al., 2008), and five known steroids, ganodermasides A (8), B (9), and D (10; Weng et al., 2010, 2011), ergosterol (11; Feng et al., 2010), and dankasterone B (12; Amagata et al., 2007; **Figure 1**). Compounds 8 and 9 exhibited cytotoxicities against human breast cancer cell line MDA-MB-231, colorectal cancer cell line HCT116, and hepatoma cell line HepG2 (**Table 3**). Compounds 9 and 10 showed antibacterial activity against marine fouling bacteria *Aeromonas salmonicida*. Here, we address the isolation, structure elucidation, and biological activity evaluation of the isolated compounds.
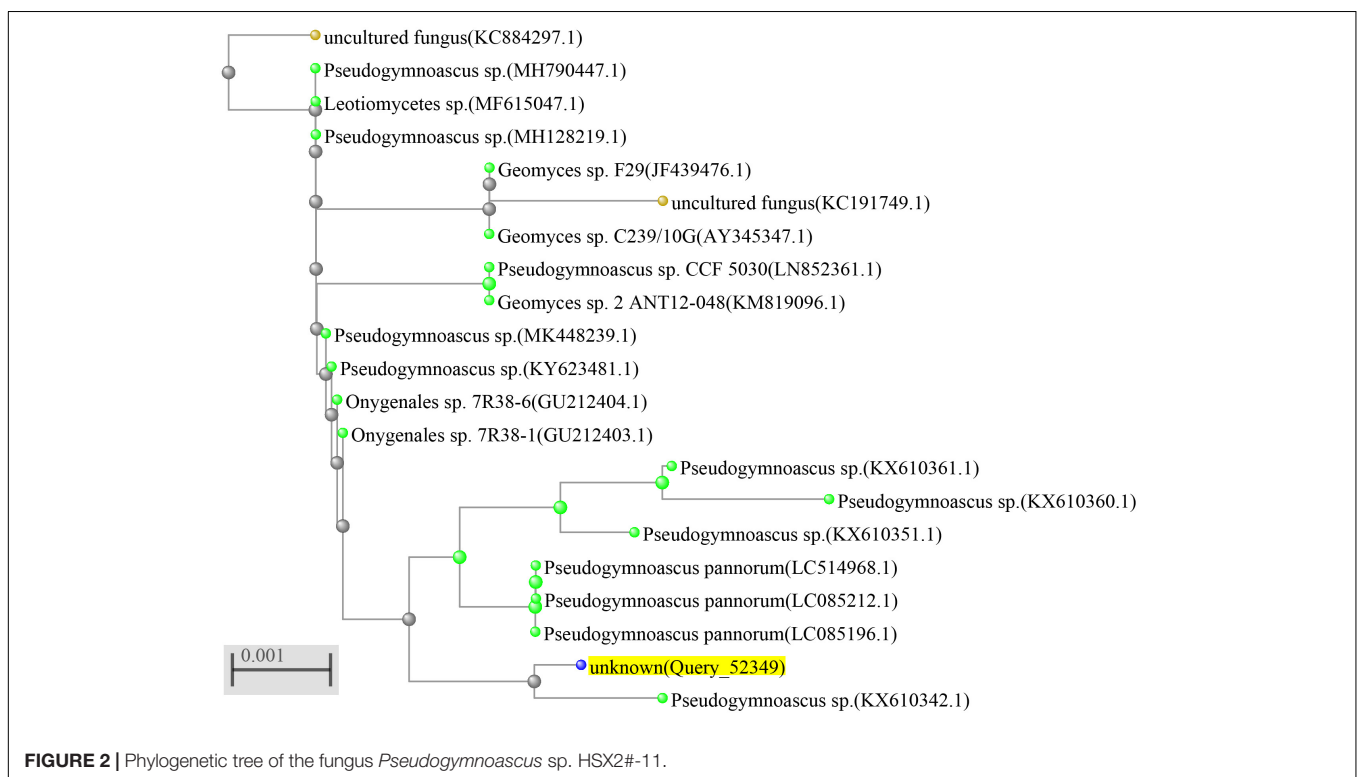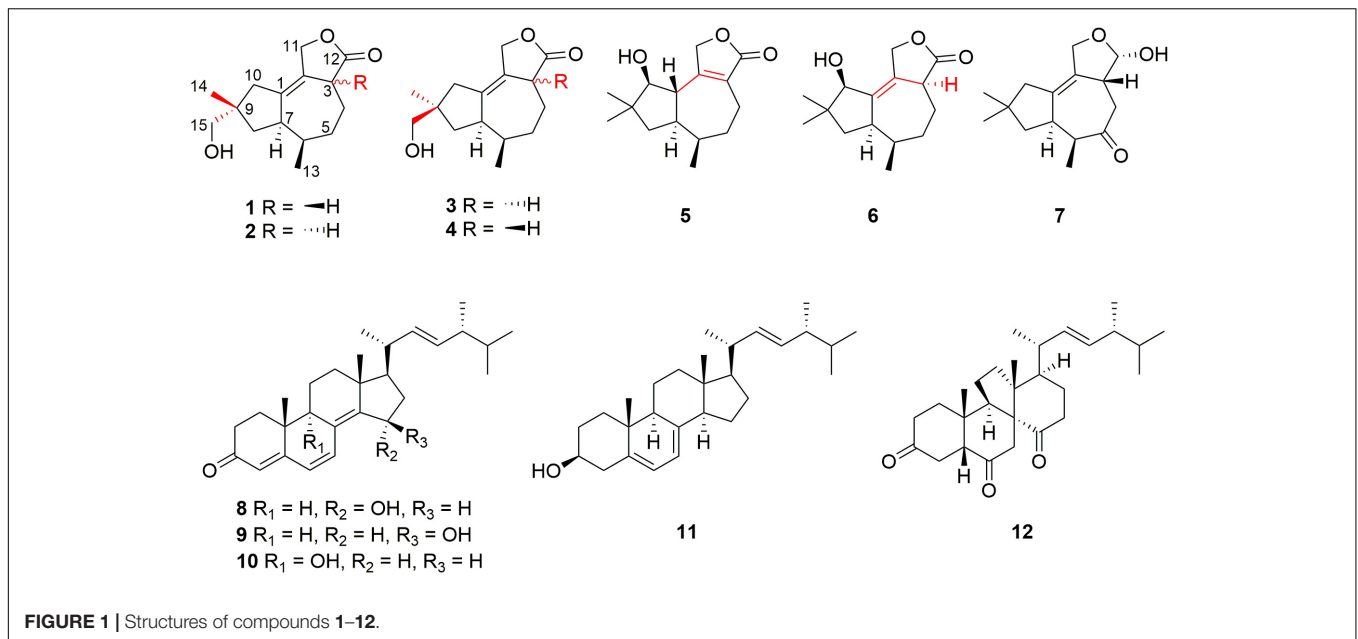
# EXPERIMENTAL SECTION

## General Experimental Procedures

Optical rotations were measured on a JASCO P-1020 digital polarimeter (JASCO, Japan). The UV spectrum was recorded using an Implen Gmbh NanoPhotometer N50 Touch (Implen, Germany). ECD spectra were obtained on a Jasco J-815-150S circular dichroism spectrometer (JASCO, Japan). NMR spectra were recorded on a Bruker AVANCE NEO (Bruker, Switzerland) at 600 MHz for $^1$H and 150 MHz for $^{13}$C in CDCl$_3$. Chemical shifts $\delta$ were recorded in ppm using TMS as the internal standard. HR-APCI-MS spectra were measured on a Thermo Scientific LTQ Orbitrap XL spectrometer (Thermo Fisher Scientific, Bremen, Germany). HPLC separation was performed using a Hitachi Primaide Organizer Semi-HPLC system (Hitachi High Technologies, Tokyo, Japan) coupled with a Hitachi Primaide 1430 photodiodearray detector (Hitachi High Technologies, Tokyo, Japan). A Kromasil C$_{18}$ semi-preparative HPLC column (250 × 10 mm, 5 μm; Eka Nobel, Bohus, Sweden) was used. Silica gel (200–300 mesh; Qingdao Marine Chemical Group Co., Qingdao, China) and Sephadex LH-20 (Amersham Biosciences Inc., Piscataway, NJ, United States) were used for column chromatography (CC). Precoated silica gel GF254 plates (20 × 20 cm, Yantai Zifu Chemical Group Co., Yantai, China).

## Fungal Materials

The soil samples were collected in ice-free areas (about 10 cm underground) of the Fields Peninsula using sterile spatulas and sterilized WhirlPak bags (Sigma-Aldrich, United States), and were transported to the lab in sealed foam package with dry ice added by airplane, at the Chinese 35th Antarctic expedition in 2019. The fungus *Pseudogymnoascus* sp. HSX2#-11 was isolated from a soil sample from Fields Peninsula. The strain was deposited at −80°C in the State Key Laboratory of Microbial Technology, Institute of Microbial Technology, Shandong University, Qingdao, China.

The identification of the fungal strain HSX2#-11 was conducted by the analysis of the 28S rRNA gene sequence. The fresh fungal mycelium (about 1.00 mg) was dispersed in a 50 μl lysis buffer for the microorganisms to direct PCR (Takara, Cat# 9164), saved in metal bath (Yooning, China) at 100°C for 30 min to extract its genomic DNA as the template DNA. The PCRs were performed in a final volume of 50 μl, which was composed of the template DNA (3 μl), ITS1 (1 μl), ITS4 (1 μl), PrimeSTAR® Max DNA Polymerase (25 μl, Takara, Cat# R045A), and ultrapure water (20 μl), under the following procedures: (1) initial denaturation at 98°C for 5 min; (2) denaturation at 98°C for 30 s; (3) annealing at 55°C for 30 s; (4) extension at 72°C for 1 min; and (5) final extension at 72°C for 10 min. Steps 2–4 were repeated 30 times. The PCR products were then submitted for sequencing (BGI, China) with the primers ITS1 and ITS4. The sequence of HSX2#-11 was searched in the NCBI nucleotide collection database through the BLAST program. The phylogenetic tree of the top 20 most similar to this fungal sequence identified the strain HSX2#-11 as

**FIGURE 1 |** Structures of compounds **1–12**.



**FIGURE 2 |** Phylogenetic tree of the fungus *Pseudogymnoascus* sp. HSX2#-11.

a *Pseudogymnoascus* sp. (**Figure 2**), with GenBank (NCBI) accession number MT367223.1.

## Extraction and Isolation

The fungal strain *Pseudogymnoascus* sp. HSX2#-11 was fermented in a PDA liquid medium in 200 Erlenmeyer flasks (300 ml in each 1,000-ml flask) at 16°C in air condition room for 45 days. The culture (60 L) was filtered to separate the broth from the mycelia. Then the mycelia were extracted three times with EtOAc (3 × 4,000 ml) and then repeatedly extracted with $CH_2Cl_2$–MeOH (v/v, 1:1) three times (3 × 4,000 ml). The broth was extracted repeatedly with EtOAc (3 × 60 L) to get the EtOAc layer. All the extracts were combined and then evaporated to dryness under reduced pressure to afford a residue (71.5 g). The residue was subjected to vacuum liquid chromatography on silica gel using step gradient elution

with EtOAc–petroleum ether (PE; 0–100%) and then with MeOH–EtOAc (0–100%) to afford eight fractions (Fr.1–Fr.8). Fr.2 was the pure compound **11** (89.7 mg). Fr.3 was first subjected to the gradient elution of ODS CC with MeOH in $H_2O$ (10–100%) and then purified by using semipreparative HPLC on an ODS column (Kromasil $C_{18}$, 250 × 10 mm, 5 μm, 2 ml/min) eluted with 85% MeOH–$H_2O$ to give compound **12** (2.7 mg). Fr.4 was isolated by CC on Sephadex LH-20 eluted with $CH_2Cl_2$–MeOH (v/v, 1:1) to afford two fractions (Fr.4.1, Fr.4.2). Fr.4.1 was subjected to silica gel CC eluting with EtOAc–PE (0–50%) to get three fractions (Fr.4.1.1–4.1.3). Fr.4.1.1 was first purified by HPLC eluted with 60% MeOH–$H_2O$ to give compound **7** (1.9 mg), and then purified by HPLC eluted with 40% MeCN–$H_2O$ to afford **5** (0.1 mg) and **6** (0.2 mg). Fr.4.1.2 was subjected on HPLC eluting with 35% MeCN–$H_2O$ to give **1** (0.7 mg) and **2** (0.7 mg). Fr.4.1.3 was separated on HPLC eluting with 30% MeCN–$H_2O$ to get **3** (0.6 mg) and **4** (0.5 mg). Fr.4.2 was first separated on silica gel CC eluting with EtOAc–PE (0–50%), and then purified by HPLC eluting with 75% MeOH–$H_2O$ to gain **8** (13.6 mg), **10** (3.1 mg), and **9** (11.1 mg).

Pseudotremulane A (**1**): colorless oil; $[\alpha]_D^{20}$ + 8.6 (c 0.058, MeOH); UV ($CH_2Cl_2$) $\lambda_{max}$ (log ε): 224 (4.90) nm; CD (3.4 mM, MeOH) $\lambda_{max}$ (Δε) 204 (+9.51), 230 (−4.31) nm; $^1$H and $^{13}$C NMR data, see **Tables 1**, **2**; HR-APCI-MS m/z 251.1641 $[M + H]^+$ (calcd for $C_{15}H_{23}O_3$, 251.1642).

Pseudotremulane B (**2**): colorless oil; $[\alpha]_D^{20}$ + 13.9 (c 0.058, MeOH); UV ($CH_2Cl_2$) $\lambda_{max}$ (log ε): 223 (4.82); CD (3.4 mM, MeOH) $\lambda_{max}$ (Δε) 223 (+4.80) nm; $^1$H and $^{13}$C NMR data, see **Tables 1**, **2**; HR-APCI-MS m/z 251.1641 $[M + H]^+$ (calcd for $C_{15}H_{23}O_3$, 251.1642).

Pseudotremulane C (**3**): colorless oil; $[\alpha]_D^{20}$ + 20.6 (c 0.050, MeOH); UV ($CH_2Cl_2$) $\lambda_{max}$ (log ε): 228 (4.48); CD (4.0 mM, MeOH) $\lambda_{max}$ (Δε) 217 (+3.05) nm; $^1$H and $^{13}$C NMR data, see **Tables 1**, **2**; HR-APCI-MS m/z 251.1642 $[M + H]^+$ (calcd for $C_{15}H_{23}O_3$, 251.1642).

Pseudotremulane D (**4**): colorless oil; $[\alpha]_D^{20}$ + 8.5 (c 0.042, MeOH); UV ($CH_2Cl_2$) $\lambda_{max}$ (log ε): 223 (4.88); CD (2.4 mM, MeOH) $\lambda_{max}$ (Δε) 205 (+13.51), 232 (−5.56) nm; $^1$H and $^{13}$C NMR data, see **Tables 1**, **2**; HR-APCI-MS m/z 251.1641 $[M + H]^+$ (calcd for $C_{15}H_{23}O_3$, 251.1642).

Pseudotremulane E (**5**): colorless oil; $[\alpha]_D^{20}$ −75.0 (c 0.008, MeOH); UV ($CH_2Cl_2$) $\lambda_{max}$ (log ε): 224 (5.51); CD (1.2 mM, MeOH) $\lambda_{max}$ (Δε) 222 (−0.29), 247 (+1.29) nm; $^1$H and $^{13}$C NMR data, see **Tables 1**, **2**; HR-APCI-MS m/z 251.1638 $[M + H]^+$ (calcd for $C_{15}H_{23}O_3$, 251.1642).

Pseudotremulane F (**6**): colorless oil; $[\alpha]_D^{20}$ + 7.9 (c 0.017, MeOH); UV ($CH_2Cl_2$) $\lambda_{max}$ (log ε): 221 (5.17); CD (6.0 mM, MeOH) $\lambda_{max}$ (Δε) 223 (+4.29) nm; $^1$H and $^{13}$C NMR data, see **Tables 1**, **2**; HR-APCI-MS m/z 251.1641 $[M + H]^+$ (calcd for $C_{15}H_{23}O_3$, 251.1642).

## Cytotoxicity Assays

Cytotoxicities against human breast cancer (MDA-MB-231), colorectal cancer (HCT116), lung carcinoma (A549), pancreatic carcinoma (PANC-1), and hepatoma (HepG2) cell lines were evaluated using the SRB method (Skehan et al., 1990).

Adriamycin was used as a positive control. The cell lines of MDA-MB-231, HCT116, A549, PANC-1, and HepG2 in the logarithmic growth phase were seeded into 96-well plates with 5,000 cells/well (100 μl/well), respectively. After 24 h of culture, the isolated compounds to be tested were added (the final concentration was shown in **Supplementary Table 1**), and three replicates were set for each concentration. The dosage of DMSO in the solvent control group was 0.1% of the maximum dose used in the test group. After 72 h of drug treatment, 10% (m/v) of cold trichloroacid acid was added to each well to fix the cells. After SRB staining, 150 μl/well Tris solution was added to determine the optic density (OD) values at 515 nm on a microplate reader (TriStar$^2$ S LB 942 Multimode Reader, Berthold Technologies, Germany). The inhibition rates of the tumor cell growth were calculated by the following formula:

$$\text{Inhibition rate (\%)} = \left(\text{OD}_{DMSO} - \text{OD}_{compound}\right) / \text{OD}_{DMSO} \times 100$$

The $IC_{50}$ values were calculated using the method of log (inhibitor) vs. normalized response in the software package GraphPad Prism 5.

## Antibacterial Activity Assays

The antibacterial activities were evaluated by the conventional broth dilution assay (Appendino et al., 2008). Nine marine fouling bacteria, *Pseudomonas fulva*, *Aeromonas hydrophila*, *A. salmonicida*, *Vibrio anguillarum*, *V. harveyi*, *Photobacterium halotolerans*, *P. angustum*, *Enterobacter cloacae*, and *E. hormaechei*, were used, and cipofloxacin was used as a positive control. The initial screening of antibacterial activity assays was tested in a 96-well plate. Each well contained 198 μl tested bacterial suspension (2–5 × 10$^5$ CFU/ml in LB broth) and 2 μl compound (final concentration was 20 μM). Three replicates were performed. The plates were incubated at 37°C for 24 h, and then the OD values were tested at 600 nm in a microplate reader (TriStar$^2$ S LB 942 Multimode Reader, Berthold Technologies, Germany). The inhibitory rates were calculated according to the following formula:

$$\text{Inhibition rate (\%)} = \left(\text{OD}_{DMSO} - \text{OD}_{compound}\right) / \text{OD}_{DMSO} \times 100$$

The MIC values of some active target compounds were evaluated using the twofold serial dilution method. The concentrations of the compounds ranged from 100 to 6.25 μM. The other steps were the same as in the primary screening. The MIC values were calculated using the method of log (inhibitor) vs. normalized response in the software package GraphPad Prism 5.

## RESULTS

## Structure Elucidations of Isolated Compounds

Pseudotremulane A (**1**) was obtained as a colorless oil. Its molecular formula, $C_{15}H_{22}O_3$, was determined by the

**TABLE 1 |** $^1$H NMR data of compounds **1–6** in CDCl$_3$ at 600 MHz.

| No. | 1 | 2 | 3 | 4 | 5 | 6 |
|---|---|---|---|---|---|---|
| 1 | | | | | 2.71, t (10.5) | |
| 3 | 3.03–2.99, m | 3.14–3.08, m | 3.15, d (12.1) | 3.03, d (12.2) | | 3.16, dt (12.1, 2.8) |
| 4 | 2.23, dd (13.5, 6.1) | 1.95, ddt (14.0, 5.3, 2.7) | 1.96, ddt (13.3, 5.5, 2.8) | 2.25, dd (14.1, 6.2) | 2.47, d (16.9) | 2.01–1.96, m |
| | 1.75, dd (13.5, 6.2) | 1.62, ddd (14.0, 12.5, 2.1) | 1.63, ddd (13.3, 12.1, 2.1) | 1.88–1.78, m | 2.38–2.29, m | 1.65, d (13.2) |
| 5 | 2.05, dd (14.2, 8.5) | 2.03–1.98, m | 2.04–1.99, m | 2.11–2.04, m | 1.71–1.62, m | 2.05–2.02, m |
| | 1.47, td (14.2, 6.2) | 1.77, dt (13.5, 2.7) | 1.81–1.79, m | 1.49, dt (13.3, 6.2) | | 1.79, t (13.2) |
| 6 | 2.11–2.07, m | 1.91–1.86, m | 1.91, dq (7.0, 3.0) | 2.17–2.11, m | 2.08–2.00, m | 1.96–1.91, m |
| 7 | 3.10–3.03, m | 2.89–2.83, m | 2.98–2.92, m | 3.16, br s | 2.08–2.00, m | 2.91–2.86, m |
| 8 | 1.82–1.77, m | 1.82–1.79, m | 1.58, t (12.0) | 1.60, t (12.0) | 1.60–1.56, m | 1.69, d (12.0) |
| | 1.41, t (12.5) | 1.40, dd (13.3, 10.7) | 1.50, dd (12.0, 8.4) | 1.42, dd (12.0, 7.3) | 1.53–1.50, m | 1.46, dd (12.0, 8.1) |
| 10 | 2.32, d (17.5) | 2.13, d (16.1) | 2.07, d (15.7) | 2.17–2.11, m | 3.64, dd (10.5, 6.2) | 3.73, s |
| | 1.90, d (17.5) | 1.86–1.82, m | 1.85–1.81, m | 2.11–2.04, m | | |
| 11 | 4.67, d (10.3) | 4.75, d (13.2) | 4.75, d (13.3) | 4.67, d (12.0) | 4.91, d (17.8) | 5.00, d (13.6) |
| | 4.65, d (10.3) | 4.69, d (13.2) | 4.68, d (13.3) | 4.62, d (12.0) | 4.81, d (17.8) | 4.88, d (13.6) |
| 13 | 0.93, d (7.2) | 0.88, d (6.9) | 0.86, d (7.0) | 0.93, d (7.1) | 0.96, d (5.8) | 0.91, d (7.0) |
| 14 | 1.11, s | 1.12, s | 0.92, s | 1.06, s | 0.95, s | 1.07, s |
| 15 | 3.46, d (10.6) | 3.30, d (10.6) | 3.52, s | 3.49, s | 1.07, s | 0.82, s |
| | 3.39, d (10.6) | 3.26, d (10.6) | | | | |

**TABLE 2 |** $^{13}$C NMR data of compounds **1–6** in CDCl$_3$ at 150 MHz.

| No. | 1 | 2 | 3 | 4 | 5 | 6 |
|---|---|---|---|---|---|---|
| 1 | 138.5, C | 138.8, C | 138.4, C | 138.0, C | 45.0, CH | 140.8, C |
| 2 | 125.0, C | 125.6, C | 125.8, C | 125.2, C | 162.9, C | 132.6, C |
| 3 | 43.56, CH | 44.5, CH | 44.6, CH | 43.6, CH | 128.8, C | 44.7, CH |
| 4 | 26.5, CH$_2$ | 22.7, CH$_2$ | 22.6, CH$_2$ | 26.5, CH$_2$ | 20.1, CH$_2$ | 22.2, CH$_2$ |
| 5 | 33.1, CH$_2$ | 36.9, CH$_2$ | 36.9, CH$_2$ | 33.2, CH$_2$ | 33.5, CH$_2$ | 36.9, CH$_2$ |
| 6 | 32.7, CH | 31.5, CH | 31.5, CH | 32.6, CH | 32.7, CH | 30.7, CH |
| 7 | 43.59, CH | 48.4, CH | 47.7, CH | 43.2, CH | 41.5, CH | 47.5, CH |
| 8 | 40.8, CH$_2$ | 40.1, CH$_2$ | 39.7, CH$_2$ | 40.6, CH$_2$ | 42.3, CH$_2$ | 41.1, CH$_2$ |
| 9 | 42.6, C | 43.8, C | 43.9, C | 42.8, C | 39.0, C | 42.6, C |
| 10 | 41.2, CH$_2$ | 41.5, CH$_2$ | 41.6, CH2 | 41.1, CH$_2$ | 83.6, CH | 80.1, CH |
| 11 | 69.20, CH$_2$ | 69.6, CH$_2$ | 69.6, CH2 | 69.2, CH$_2$ | 71.1, CH$_2$ | 68.9, CH2 |
| 12 | 177.8, C | 179.3, C | 179.3, C | 177.8, C | 175.3, C | 178.6, C |
| 13 | 17.5, CH$_3$ | 12.0, CH$_3$ | 12.1, CH$_3$ | 17.7, CH$_3$ | 12.1, CH$_3$ | 12.9, CH$_3$ |
| 14 | 24.3, CH$_3$ | 23.6, CH$_3$ | 22.7, CH$_3$ | 23.2, CH$_3$ | 23.9, CH$_3$ | 22.1, CH$_3$ |
| 15 | 69.18, CH$_2$ | 68.9, CH$_2$ | 71.2, CH$_2$ | 71.5, CH$_2$ | 29.1, CH$_3$ | 25.7, CH$_3$ |

**TABLE 3 |** Cytotoxicities (IC$_{50}$, μM) of compounds **8** and **9**.

| Compounds | 8 | 9 |
|---|---|---|
| MDA-MB-231 | 30 ± 2.0 | 27 ± 1.7 |
| A549 | >40 | >40 |
| HCT116 | 25 ± 1.5 | 23 ± 0.93 |
| HepG2 | 21 ± 1.0 | 23 ± 1.3 |
| PANC-1 | >40 | >40 |

HR-APCI-MS spectrum (**Supplementary Figure 7**), with five degrees of unsaturation. The analysis of $^1$H NMR and $^{13}$C NMR spectra (**Supplementary Figures 1**, **2**) combined with the HSQC spectrum (**Supplementary Figure 3**) of **1** indicated two methyl signals at $\delta_H$ 0.93 (3H, d, 7.2 Hz), $\delta_C$ 17.5; $\delta_H$ 1.11 (3H, s), $\delta_C$ 24.3, six methylenes, including two oxygenated methylenes at $\delta_H$ 3.39 (1H, d, 10.6 Hz), 3.46 (1H, d, 10.6 Hz), $\delta_C$ 69.18; $\delta_H$ 4.65 (1H, d, 10.3 Hz), 4.67 (1H, d, 10.3 Hz), $\delta_C$ 69.20, three methines, and four quaternary carbon signals, including two olefinic carbons at $\delta_C$ 125.0 and $\delta_C$ 138.5, and one ester group at $\delta_C$ 177.8, which represented two degrees of unsaturation (**Tables 1**, **2**). The other degrees of unsaturation revealed that there had been three rings in the structure of **1**. These data suggested that **1** was tremulane-type sesquiterpenoid similar to 11,12-epoxy-12$\beta$-hydroxy-1-tremulen-5-one (**7**; Zhou et al., 2008). There had been three obvious differences between **1** and **7**. The disappeared ketone carbonyl in **7** was replaced by the arisen methylene at C-5 in **1** (**Tables 1**, **2**); this was further confirmed by the key HMBC correlation from H-13 to C-5 (**Figure 3**). The HMBC correlations from H-11 to C-12, and H-4 to C-12 indicated the

**FIGURE 3 |** Key COSY and HMBC correlations of compounds **1**–**6**.



**FIGURE 4 |** Key NOESY correlations of compounds **1**–**4** and **6**.
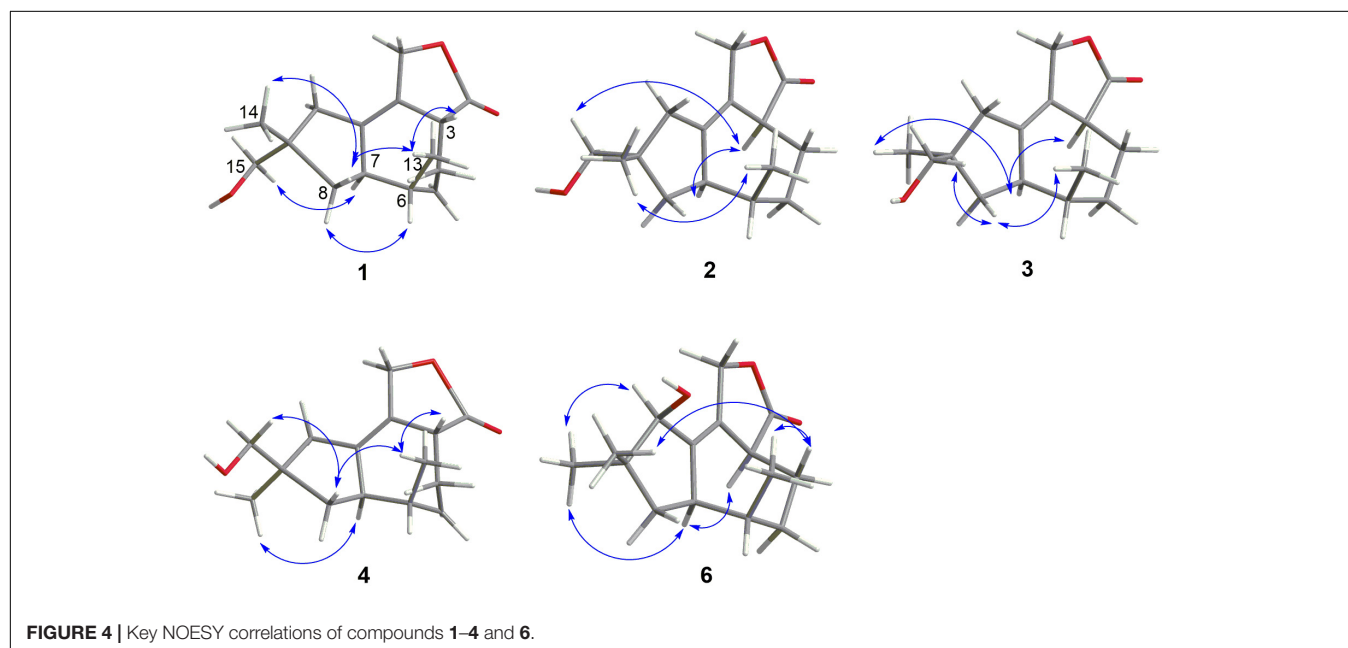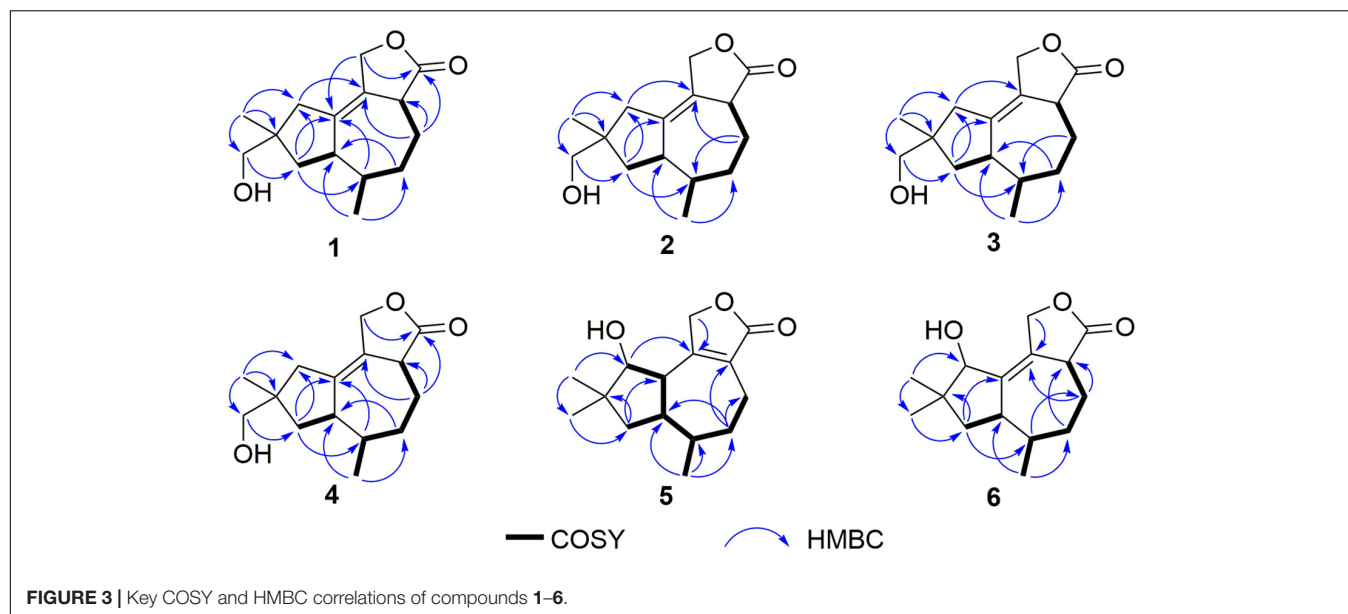
ester group carbon at C-12 (**Figure 3**). The lower field shift of C-15 data (**Tables 1**, **2**) compared with those of **7**, combined with the HMBC correlations from H-15 to C-8, and H-14 to C-15 elucidated the oxidation of C-15 (**Figure 3**). Thus, the planer structure of **1** was unambiguously confirmed. The relative configurations of **1** were determined by NOESY spectra analysis (**Supplementary Figure 6**). The NOESY correlations between H-14 and H-8b, H-8b and H-13, and H-13 and H-3 indicated that H-14, H-13, and H-3 were in the same orientation (**Figure 4**). The other orientation of H-6, H-7, and H-15 was suggested by the NOESY cross-peaks of H-6/H-8a and H-7/H-15 (**Figure 4**). Therefore, the relative configurations of **1** were assigned as 3R*,6R*,7R*,9S*.

Pseudotremulane B (**2**) was gained as a colorless oil, with the molecular formula of $C_{15}H_{22}O_3$ determined by HR-APCI-MS indicating five degrees of unsaturation and had the same molecular formula as **1** (**Supplementary Figure 14**). The $^1H$ and $^{13}C$ NMR data of **2** were very similar to those of **1** (**Tables 1**, **2**). The downfield shift of C-2, C-3, C-5, C-7, C-9, C-11, and C-12 and the high-field shift of C-4, C-6, C-8, C-13, and C-14 in $^{13}C$ NMR suggested the difference configurations between **1** and **2**. The NOESY cross-peaks of H-15/H-3 and H-3/H-7 declared that H-3, H-7, and H-15 were in the same face (**Figure 4**). The NOESY correlation of H-13 and H-14 indicated that H-13 and H-14 were in another face. Therefore, the relative configurations of **2** were assigned as 3S*,6R*,7R*,9S*.

Pseudotremulane C (**3**) was acquired as a colorless oil. The HR-APCI-MS of **3** exhibited the same molecular formula with **1** and **2** (**Supplementary Figure 21**). The strong similar ^{1}H and ^{13}C NMR data between **2** and **3** (**Tables 1, 2**) suggested that they shared the same planer structures. The high-field shift of C-14 and the downfield shift of C-15 (**Table 2**) revealed the difference configurations of C-9 of **2** and **3**. The $\alpha$-orientation of H-3, H-7, and H-14 was determined by the NOESY correlations of H-3/H-7 and H-7/H-14 (**Figure 4**). The $\beta$-orientation of H-13 and H-15 was determined by the NOESY cross-peaks of H-13/H-8a and H-8a/H-15 (**Figure 4**). Compounds **2** and **3** were a pair of epimeride at the location of C-9.

Pseudotremulane D (**4**) was obtained as a colorless oil, with the same molecular formula with **1–3**, according the analysis of its HR-APCI-MS spectrum (**Supplementary Figure 28**). Careful analysis of the ^{1}H and ^{13}C NMR data of **1** and **4** indicated that they had the same planer structures. The difference configurations of C-9 of **1** and **4** were determined by the high-field shift of C-14 and the downfield shift of C-15 (**Table 2**). The NOESY correlations of H-3/H-13, H-13/H-8a, and H-8a/H-15 (**Figure 4**) revealed the $\beta$-orientation of H-3, H-13, and H-15. The $\alpha$-orientation of H-7 and H-14 was proved by the NOESY cross-peak of H-7/H-14 (**Figure 4**). Compounds **1** and **4** were a pair of epimeride at the location of C-9.

Pseudotremulane E (**5**) was obtained as a colorless oil. Its molecular formula was the same as **1–4**, as suggested by HR-APCI-MS (**Supplementary Figure 35**). The NMR spectra of **5** revealed the presence of three methyls, four methylenes (one oxygenated), four methines (one oxygenated), and four quaternary carbons (one ester group carbon, two olefinic, and one sp[3] quaternary carbon; **Supplementary Figures 29–31**). These characteristic NMR spectroscopic data of **5** showed similarities with those of 11,12-epoxy-12$\beta$-hydroxy-1-tremulen-5-one (**7**; Zhou et al., 2008). Compared with **7**, the disappeared ketone at C-5 was substituted by methylene [$\delta_H$ 1.71–1.62 (2H, m), $\delta_C$ 33.5] in **5** (**Tables 1, 2**), elucidated by the ^{1}H-^{1}H COSY correlations of H-6/H-5 and H-5/H-4, and further confirmed by the HMBC correlations from H-13 to C-5, and H-5 to C-3, C-4, and C-7 (**Figure 3**). The position of the double bond was changed from C-1/C-2 in **7** into C-2/C-3 in **5**, proved by the ^{1}H-^{1}H COSY cross-peak of H-1/H-7 and the HMBC signals of H-10/C-2, H-11/C-2, and H-5/C-3 (**Figure 3**). The absence of carbonyl carbon ($\delta_C$ 175.3) in **5** and the disappeared oxygenated methine at C-12 in **7**, combined with the molecular formula of **5**, revealed that there had been an ester group at C-12 in **5**. The large coupling constants of H-1/H-10 (J = 11.0 Hz) and H-1/H-7 (J = 11.0 Hz) revealed the $\beta$-orientation of H-1 and the $\alpha$-orientation of H-7 and H-10 (**Table 1**). The overlapped ^{1}H NMR signals of H-6/H-7 and H-13/H-14 increased the difficulties to decide the configurations of **5** (**Table 1**). However, based on biogenetic considerations, H-13 was proposed to have $\beta$-orientation be the same with **1–6**.

Pseudotremulane F (**6**) was isolated as a colorless oil. The same molecular formula of $C_{15}H_{22}O_3$ was determined by the HR-APCI-MS spectrum (**Supplementary Figure 42**). The three methyls, four methylenes (one oxygenated), four methines (one oxygenated), and four quaternary carbons (one ester group carbon, two olefinic, and one sp[3] quaternary carbon) exhibited
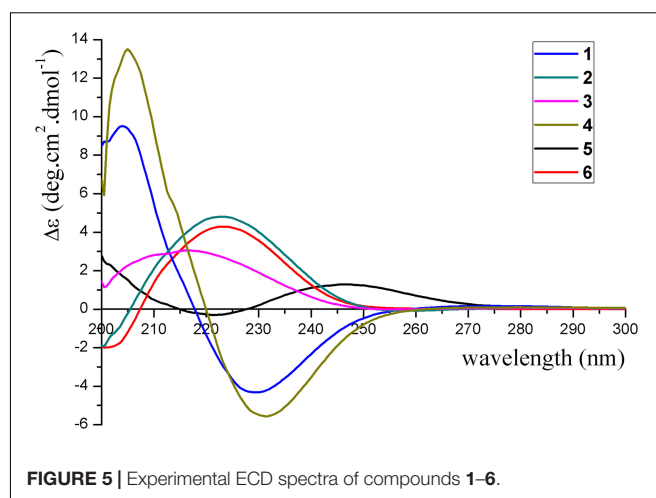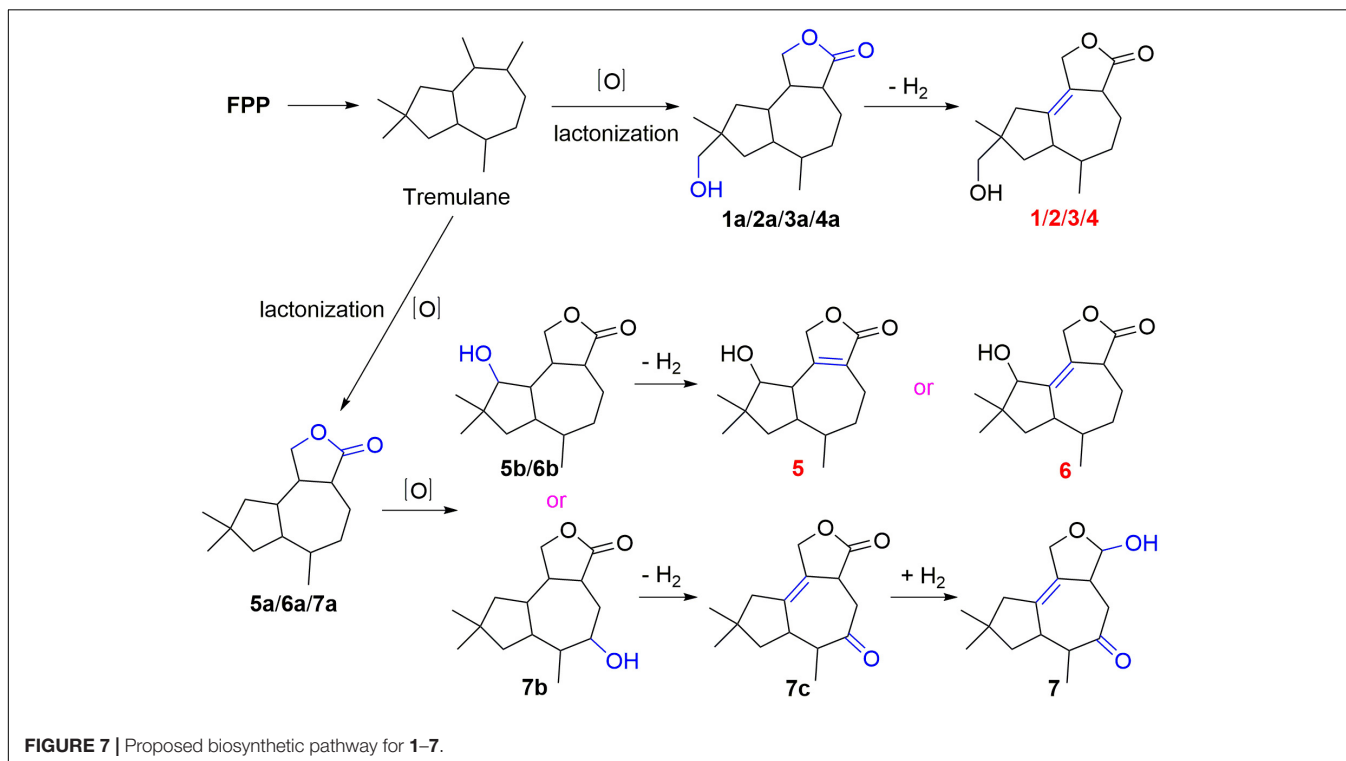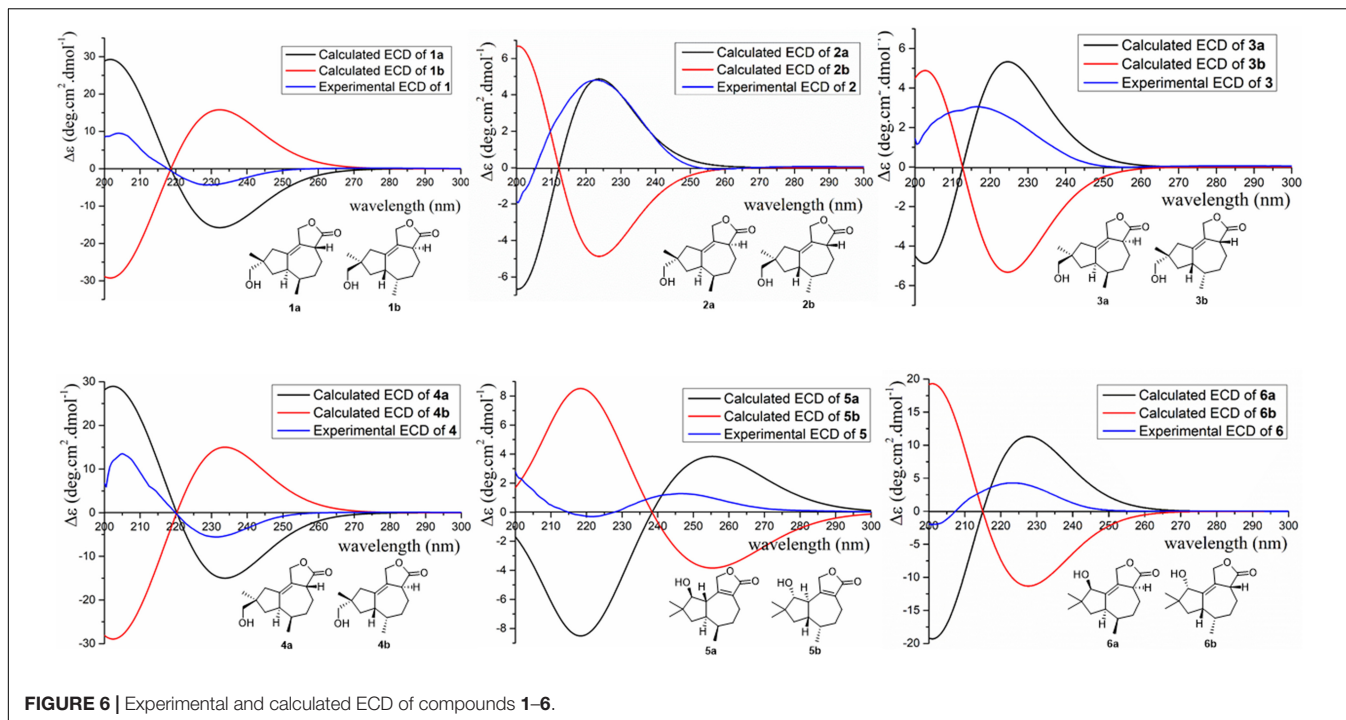


**FIGURE 5** | Experimental ECD spectra of compounds **1–6**.

in the NMR spectra (**Supplementary Figures 29–31**), indicating the similar structures of **6** and **5**. The most obvious differences of ^{13}C NMR data between **6** and **5** were the downfield shift of C-1 ($\delta_C$ 140.8 in **6** vs $\delta_C$ 45.0 in **5**) and the high-field shift of C-2 ($\delta_C$ 132.6 in **6** vs $\delta_C$ 162.9 in **5**) and C-3 ($\delta_C$ 44.7 in **6** vs $\delta_C$ 128.8 in **5**; **Table 2**), elucidating that the olefinic bond location was changed from C-2/C-3 in **5** into C-1/C-2 in **6**. This was further confirmed by the HMBC correlations from H-11 to C-2, H-4 to C-2, and H-8 to C-1 (**Figure 3**). The $\beta$-orientation of H-13 and H-14 was revealed by the NOESY cross-peaks of H-13/H-4b and H-4b/H-14, and the $\alpha$-orientation of H-3, H-7, H-15, and H-10 was suggested by the NOESY correlations of H-3/H-7, H-7/H-15, and H-15/H-10 (**Figure 4**).

The absolute configurations of **1–6** were determined by their ECD spectra (**Figure 5**) and were further confirmed by ECD calculations. The experimental ECD spectrum of **1** exhibited a negative cotton effect at 230 nm. According to the $\pi$-$\pi^*$ CD octant rule for olefins (Guo et al., 2016), the negative cotton effect at 230 nm was caused by ester carbonyl (C-12) and oxymethene (C-11) lying in the negative contribution region (**Figure 5**). Combined with the relative configuration conclusions, the absolute configurations of **1** were established as 3R,6R,7R,9S, and named as pseudotremulane A. The similar ECD spectra of **4** and **5** with the negative cotton effects at 232 and 222 nm (**Figure 5**), respectively, indicated the absolute configurations of 3R,6R,7R,9R–**4** and 1S,6R,7R,10S–**5**. The positive cotton effects of the ECD spectra of compounds **2** (223 nm), **3** (217 nm), and **6** (223 nm) elucidated the absolute configurations of 3S,6R,7R,9S–**2**, 3S,6R,7R,9R–**3**, and 3S,6R,7R,10R–**6** (**Figure 5**). Thus, the structures compounds **2–6** were completely confirmed and named as pseudotremulanes B-F, respectively.

To further conform these results, the theoretical ECDs of compounds **1–6** (**Figure 6**) were calculated to compare with their experimental ECD spectra (Mazzeo et al., 2013; Cao et al., 2020). The MMFF94S method was used to conformational searches of **1a–6a** to obtain the lowest energy conformers with relative energies between 0 and 10 kcal/mol. Gaussian 09 package was used to optimize the searched conformations. The first optimization was set at the gas-phase RB3LYP/6-31G(d) level to

**FIGURE 6** | Experimental and calculated ECD of compounds **1**–**6**.



**FIGURE 7** | Proposed biosynthetic pathway for **1**–**7**.

get preferential conformations with the relative energies less than 2.5 kcal/mol. Then the conformers were optimized again at the set of gas-phase B3LYP/6-311 + G(d). The total 60 electronic excited states were calculated at the set of gas-phase RB3LYP/6-311 + + G(2d,p). Boltzmann statistics were used to simulate

ECD with a standard deviation of σ 0.4 eV. The theoretical ECD spectra of **1b**–**6b** were obtained by directly reversing the spectra of **1a**–**6a**, respectively. The results exhibited that the experimental ECDs of **1**–**6** were matched well with the calculated ECDs of **1a**–**6a**, respectively, which further verified the absolute structures of

**FIGURE 8 |** Inhibition rates of tested cell lines of compounds **8** and **9**.
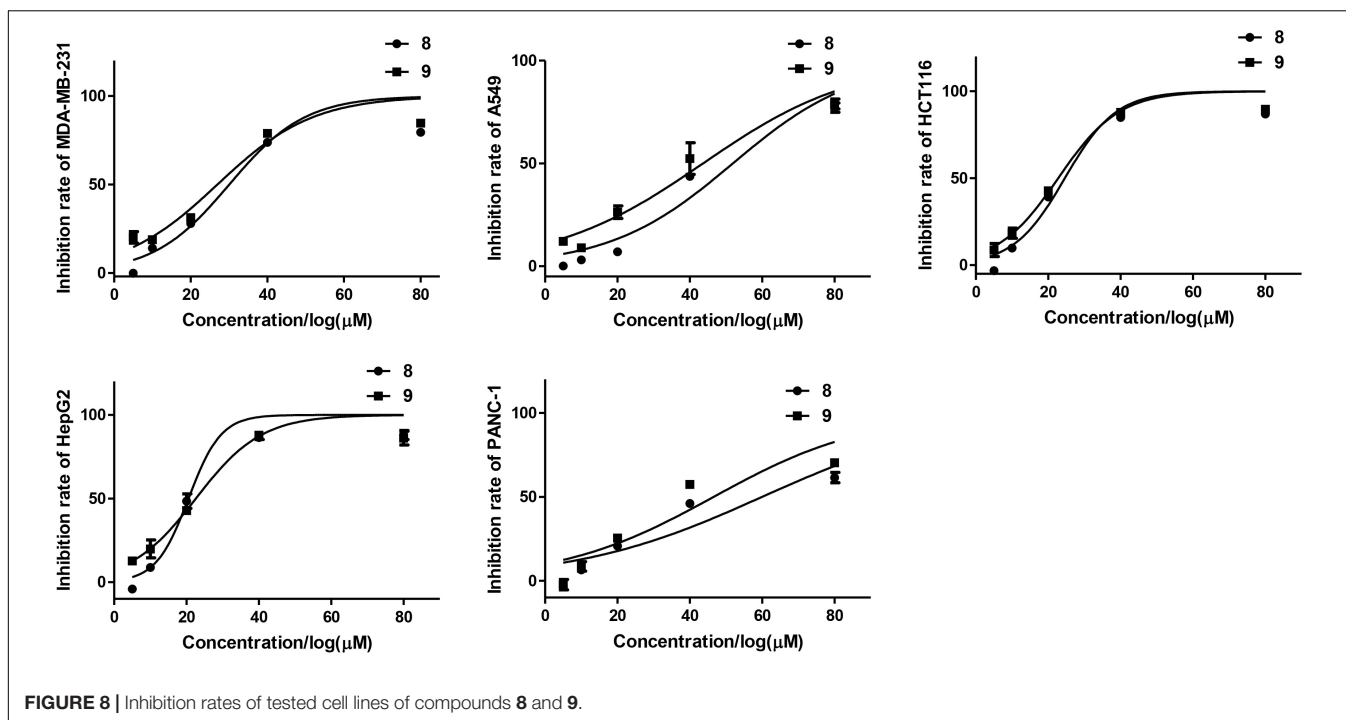
**1–6** (**Figure 6**). Interestingly, compounds **1/2**, **3/4**, **1/4**, and **2/3** were identified as four pairs of epimeride at the locations of C-3, C-3, C-9, and C-9, respectively.

The structures of **7–12** were determined as 11,12-epoxy-12$\beta$-hydroxy-1-tremulen-5-one (Zhou et al., 2008), ganodermasides A, B, and D (Weng et al., 2010, 2011), ergosterol (Feng et al., 2010), and dankasterone B (Amagata et al., 2007), respectively, by comparing their NMR data with those in the literature.

## Proposed Biosynthetic Pathway for 1–7

Compounds **1–7** could derive from tremulane, a 5/7 endocyclic system sesquiterpenoid (**Figure 7**; He et al., 2020; Wang et al., 2020). As exhibited in **Figure 7**, compounds **1–7** could be obtained after a series of oxidation, lactonization, dehydrogenation, and revivification of tremulane. The intermediate products **1a/2a/3a/4a** were obtained after the oxidation of tremulane at C-11, C-12, and C-15 and lactonization at C-11 and C-12. Then the dehydrogenation of the intermediate products at C-1 and C-2 acquired the compounds **1–4**. Similarly, compounds **5**, **6**, and **7c** were gained from tremulane after the reactions of oxidation, lactonization, and dehydrogenation. Compound **7** was obtained from the revivification of **7c**.

## Bioactivity Evaluations of Isolated Compounds

All the isolated compounds (**1–12**) were evaluated for their cytotoxic activities against five human cancer cell lines (MDA-MB-231, HCT116, HepG2, A549, and PANC-1). Compounds **8** and **9** exhibited cytotoxicities against MDA-MB-231, HCT116, and HepG2 cell lines with the IC$_{50}$ values ranging from 21 to 30 $\mu$M (**Table 3** and **Figure 8**).



**FIGURE 9 |** Inhibition rates of *A. salmonicida* of compounds **9** and **10**.
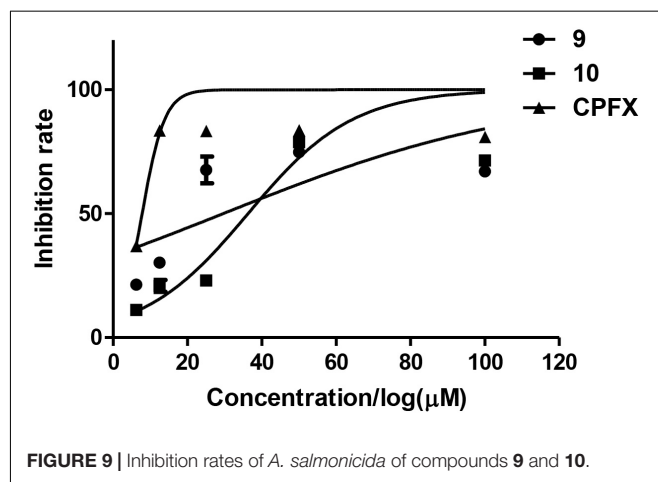
The antibacterial activities of the isolated compounds (**1–12**) were also evaluated against nine marine fouling bacteria *P. fulva*, *A. hydrophila*, *A. salmonicida*, *V. anguillarum*, *V. harveyi*, *P. halotolerans*, *P. angustum*, *E. cloacae*, and *E. hormaechei*. Compounds **9** and **10** showed antibacterial activities against marine fouling bacteria *A. salmonicida* with the MIC values of 30 and 36 $\mu$M, respectively (**Figure 9**). The MIC value of the positive control ciprofloxacin (CPFX) was 7.8 $\mu$M (**Figure 9**).

## CONCLUSION

In summary, six new tremulane sesquiterpenoids, pseudotremulanes A–F (**1–6**), together with one known analog, 11,12-epoxy-12$\beta$-hydroxy-1-tremulen-5-one (**7**), and

five known steroids, ganodermasides A (**8**), B (**9**), and D (**10**), ergosterol (**11**), and dankasterone B (**12**), were isolated from the Antarctic-derived fungus *Pseudogymnoascus* sp. HSX2#-11. Compounds **1**–**7** were proved to be isomeride structures with the same chemical formula. Compounds **1** and **2**, **3** and **4**, **1** and **4**, and **2** and **3** were identified as four pairs of epimeride at the locations of C-3, C-3, C-9, and C-9, respectively. Compounds **8** and **9** exhibited cytotoxicities against MDA-MB-231, HCT116, and HepG2 cell lines. Compounds **9** and **10** showed antibacterial activities against marine fouling bacteria *A. salmonicida*. This is the first time to discover terpenoids and steroids from the fungal genus *Pseudogymnoascus*. Our chemical investigation of the Antarctic fungus *Pseudogymnoascus* sp. HSX2#-11 enriches the chemical diversity of this fungal species.

## DISCUSSION

The genus *Pseudogymnoascus* as a kind of psychrophilic pathogenic fungi is widely distributed in Antarctica (Rosa et al., 2020; Santos et al., 2020; Martorell et al., 2021). *Pseudogymnoascus* can be one of the antagonistic fungi against potato scab pathogens from potato field soils, which could be used as potential agents to control potato scab disease (Tagawa et al., 2010). *Pseudogymnoascus* spp. has been certified to be one of the predominant microbial colonizers in the root endosphere and rhizosphere of turfgrass systems (Xia et al., 2021). The extracts of some *Pseudogymnoascus* strains exhibit potent bioactivities, such as antimicrobial, herbicidal, and antitumoral activities (Henríquez et al., 2014; Gonçalves et al., 2015; Gomes et al., 2018; Ferrarezi et al., 2019). To the best of our knowledge, only 22 natural products, including 6 new compounds, were discovered from *Pseudogymnoascus* up to now (Figueroa et al., 2015; Guo et al., 2019; Fujita et al., 2021; Shi et al., 2021). More than 70% of the previously isolated structures belong to polyketides; others are alkaloids (13.6%), benzene derivative (9.1%), and fatty acid (4.5%). Our research isolated 12 natural products (**1**–**12**), including 6 new compounds (**1**–**6**), from the fungus *Pseudogymnoascus* 2#-11. All of the isolated compounds are first obtained from the genus *Pseudogymnoascus*. This is the first time to discover terpenoids and steroids from the genus *Pseudogymnoascus*. The whole number of the fungal strain secondary metabolites increased by 35%, and the number of their new compounds is doubled. This greatly enriches the number and diversity of natural products of the genus *Pseudogymnoascus*. Except for antimicrobial activities of some of the previously obtained polyketides (Figueroa et al., 2015; Fujita et al., 2021; Shi et al., 2021), no other activities were found in *Pseudogymnoascus* in previous studies. This study is the first to identify secondary metabolites with cytotoxic activities (**8** and **9**) in *Pseudogymnoascus*.

The isolated new sesquiterpenoids (**1**–**6**), with characteristic structures of 5/7 fused bicyclic system, belong to the family of tremulanes. Tremulane derivatives have been found from cultures of *Phellinus tremulae* (Ayer and Cruz, 1993), *P. igniarius* (Liu et al., 2007; Wu et al., 2020), *Conocybe siliginea* (Zhou et al., 2008; Wu et al., 2010; He et al., 2020), *Huperzia serrata*

(Ying et al., 2013), *Flavodon flavus* (Isaka et al., 2016), *Coriolopsis* sp. (Chen et al., 2017), *Colletotrichum capsici* (Wang et al., 2017), *I. lacteus* (Chen et al., 2018, 2020; Ding et al., 2018, 2019, 2020a,b; Zhou et al., 2018; Duan et al., 2019; Wu et al., 2019; Shi et al., 2020; Sun C.-T. et al., 2020; Wang et al., 2020), and *Gymnopilus junonius* (Lee et al., 2020). This is the first time to find tremulane derivatives from *Pseudogymnoascus*.

## DATA AVAILABILITY STATEMENT

The datasets presented in this study can be found in online repositories. The names of the repository/repositories and accession number(s) can be found in the article/**Supplementary Material**.

## AUTHOR CONTRIBUTIONS

TS contributed to experimental design and operation, data analysis, and manuscript preparation. X-QL contributed to manuscript revision. LZ supported the sample of the Antarctic soil. Y-HZ contributed to ECD calculations. J-JD contributed to activity evaluations. E-LS contributed to software drawing guidance. Y-YY, Y-TZ, and W-PH contributed to activity evaluations. D-YS was the project leader organizing and guiding the experiments. All authors contributed to the article and approved the submitted version.

## FUNDING

## ACKNOWLEDGMENTS

## SUPPLEMENTARY MATERIAL

The Supplementary Material for this article can be found online at: https://www.frontiersin.org/articles/10.3389/fmicb.2021.688202/full#supplementary-material

# REFERENCES

Amagata, T., Tanaka, M., Yamada, T., Doi, M., Minoura, K., Ohishi, H., et al. (2007). Variation in cytostatic constituents of a sponge-derived *Gymnascella dankaliensis* by manipulating the carbon source. *J. Nat. Prod.* 70, 1731–1740. doi: 10.1021/np070165m

Appendino, G., Gibbons, S., Giana, A., Pagani, A., Grassi, G., Stavri, M., et al. (2008). Antibacterial cannabinoids from *Cannabis sativa*: a structure-activity study. *J. Nat. Prod.* 71, 1427–1430.

Ayer, W. A., and Cruz, E. R. (1993). The tremulanes, a new group of sesquiterpenes from the aspen rotting fungus *Phellinus tremulae*. *J. Org. Chem.* 58, 7529–7534.

Cao, F., Meng, Z.-H., Wang, P., Luo, D.-Q., and Zhu, H.-J. (2020). Dipleosporalones A and B, dimeric azaphilones from a marine-derived *Pleosporales* sp. fungus. *J. Nat. Prod.* 83, 1283–1287.

Chen, H.-P., Ji, X., Li, Z.-H., Feng, T., and Liu, J.-K. (2020). Irlactane and tremulane sesquiterpenes from the cultures of the medicinal fungus *Irpex lacteus* HFG1102. *Nat. Prod. Bioprospect.* 10, 89–100. doi: 10.1007/s13659-020-00239-z

Chen, H.-P., Zhao, Z.-Z., Li, Z.-H., Feng, T., and Liu, J.-K. (2018). Seco-tremulane sesquiterpenoids from the cultures of the medicinal Fungus *Irpex lacteus* HFG1102. *Nat. Prod. Bioprospect.* 8, 113–119. doi: 10.1007/s13659-018-0157-y

Chen, L.-L., Kong, F.-D., Wang, P., Yuan, J.-Z., Guo, Z.-K., Wang, H., et al. (2017). Two new tremulane sesquiterpenes from a mangrove endophytic fungus *Coriolopsis* sp. J5. *Chin. Chem. Lett.* 28, 222–225. doi: 10.1016/j.cclet.2016.07.019

Cong, B., Yin, X., Deng, A., Shen, J., and Yang, H. (2020). Diversity of cultivable microbes from soil of the Fildes Peninsula, Antarctica, and their potential application. *Front. Microbiol.* 11:570836. doi: 10.3389/fmicb.2020.570836

Ding, J.-H., Li, Z.-H., Feng, T., and Liu, J.-K. (2018). Tremulane sesquiterpenes from cultures of the basidiomycete *Irpex lacteus*. *Fitoterapia* 125, 245–248. doi: 10.1016/j.fitote.2017.12.001

Ding, J.-H., Li, Z.-H., Feng, T., and Liu, J.-K. (2019). A new tremulane sesquiterpenoid from the fungus *Irpex lacteus*. *Nat. Prod. Res.* 33, 316–320. doi: 10.1080/14786419.2018.1448816

Ding, J.-H., Li, Z.-H., Feng, T., and Liu, J.-K. (2020a). A sesquiterpene lactone from *Irpex lacteus*. *Chem. Nat. Compd.* 56, 403–405. doi: 10.1007/s10600-020-03047-6

Ding, J.-H., Li, Z.-H., Feng, T., and Liu, J.-K. (2020b). Two new sesquiterpenes from cultures of the fungus *Irpex lacteus*. *J. Asian Nat. Prod. Res.* 23, 348–352. doi: 10.1080/10286020.2020.1737857

Duan, X.-X., Qin, D., Song, H.-C., Gao, T.-C., Zuo, S.-H., Yan, X., et al. (2019). Irpexlacte A-D, four new bioactive metabolites of endophytic fungus *Irpex lacteus* DR10-1 from the waterlogging tolerant plant *Distylium chinense*. *Phytochem. Lett.* 32, 151–156. doi: 10.1016/j.phytol.2019.06.001

Feng, N., Zhang, J., Tang, Q., Hao, R., Liu, Y., Yang, Y., et al. (2010). Steroids from fruiting bodies of *Coprinus comatus* and their inhibition to tumor cell proliferation. *Junwu Xuebao* 29, 249–253.

Ferrarezi, J. H., Dos Santos, J. A., Sette, L. D., Ferreira, H., and Sass, D. C. (2019). Anti-*Xanthomonas* activity of Antarctic fungi crude extracts. *Afr. J. Biotechnol.* 18, 713–718. doi: 10.5897/ajb2019.16886

Figueroa, L., Jiménez, C., Rodríguez, J., Areche, C., Chávez, R., Henríquez, M., et al. (2015). 3-Nitroasterric acid derivatives from an Antarctic sponge-derived *Pseudogymnoascus* sp. fungus. *J. Nat. Prod.* 78, 919–923.

Fujita, K., Ikuta, M., Nishimura, S., Sugiyama, R., Yoshimura, A., and Kakeya, H. (2021). Amphiol, an antifungal fungal pigment from *Pseudogymnoascus* sp. PF1464. . *J. Nat. Prod.* 84, 986–992. doi: 10.1021/acs.jnatprod.0c01010

Gomes, E. C. Q., Godinho, V. M., Silva, D. A. S., de Paula, M. T. R., Vitoreli, G. A., Zani, C. L., et al. (2018). Cultivable fungi present in Antarctic soils: taxonomy, phylogeny, diversity, and bioprospecting of antiparasitic and herbicidal metabolites. *Extremophiles* 22, 381–393. doi: 10.1007/s00792-018-1003-1

Gonçalves, V. N., Carvalho, C. R., Johann, S., Mendes, G., Alves, T. M. A., and Zani, C. L. (2015). Antibacterial, antifungal and antiprotozoal activities of fungal communities present in different substrates from Antarctica. *Polar Biol.* 38, 1143–1152. doi: 10.1007/s00300-015-1672-5

Guo, Y.-Z., Wei, Q., Gao, J., Liu, B.-Y., Zhang, T., Hua, H.-M., et al. (2019). Metabolites of the psychrophilic fungus *Pseudogymnoascus pannorum*. *Nat. Prod. Res. Dev.* 31, 446–449.

Guo, Z., Li, X., Zhang, L., Feng, Z., Deng, Z., He, H., et al. (2016). Cytotoxic tremulanes and 5,6-secotremulanes, four new sesquiterpenoids from a plant-associated fungus X1-2. *Nat. Prod. Res.* 30, 2582–2589. doi: 10.1080/14786419.2015.1135140

He, J., Pu, C.-J., Wang, M., Li, Z.-H., Feng, T., Zhao, D.-K., et al. (2020). Conosiligins A-D, ring-rearranged tremulane sesquiterpenes from *Conocybe siliginea*. *J. Nat. Prod.* 83, 2743–2748. doi: 10.1021/acs.jnatprod.0c00681

Henríquez, M., Vergara, K., Norambuena, J., Beiza, A., Maza, F., Ubilla, P., et al. (2014). Diversity of cultivable fungi associated with Antarctic marine sponges and screening for their antimicrobial, antitumoral and antioxidant potential. *World J. Microbiol. Biotechnol.* 30, 65–76. doi: 10.1007/s11274-013-1418-x

Isaka, M., Palasarn, S., Supothina, S., Srichomthong, K., and Choeyklin, R. (2016). Seco-tremulanes from cultures of the basidiomycete *Flavodon flavus* BCC 17421. *Helv. Chim. Acta* 99, 232–236. doi: 10.1002/hlca.201500249

Kwon, J., Lee, H., Ko, W., Kim, D. C., Kim, K. W., Kwon, H. C., et al. (2017). Chemical constituents isolated from Antarctic marine-derived *Aspergillus* sp. SF-5976 and their anti-inflammatory effects in LPS-stimulated RAW 264.7 and BV2 cells. *Tetrahedron* 73, 3905–3912.

Lee, S., Ryoo, R., Choi, J. H., Kim, J.-H., Kim, S.-H., and Kim, K. H. (2020). Trichothecene and tremulane sesquiterpenes from a hallucinogenic mushroom *Gymnopilus junonius* and their cytotoxicity. *Arch. Pharm. Res.* 43, 214–223. doi: 10.1007/s12272-020-01213-6

Liu, D. Z., Wang, F., and Liu, J. K. (2007). Sesquiterpenes from cultures of the basidiomycete *Conocybe siliginea*. *J. Nat. Prod.* 70, 1503–1506.

Loperena, L., Soria, V., Varela, H., Lupo, S., Bergalli, A., Guigou, M., et al. (2012). Extracellular enzymes produced by microorganisms isolated from maritime Antarctica. *World J. Microbiol. Biotechnol.* 28, 2249–2256. doi: 10.1007/s11274-012-1032-3

Martorell, M. M., Lannert, M., Matula, C. V., Quartino, M. L., de Figueroa, L. I. C., MacCormack, W. P., et al. (2021). Studies toward the comprehension of fungal-macroalgae interaction in cold marine regions from a biotechnological perspective. *Fungal Biol.* 125, 218–230. doi: 10.1016/j.funbio.2020.11.003

Mazzeo, G., Santoro, E., Andolfi, A., Cimmino, A., Troselj, P., Petrovic, A. G., et al. (2013). Absolute configurations of fungal and plant metabolites by chiroptical methods. ORD, ECD, and VCD studies on phyllostin, scytolide, and oxysporone. *J. Nat. Prod.* 76, 588–599.

Poveda, G., Gil-Durán, C., Vaca, I., Levicán, G., and Chávez, R. (2018). Coldactive pectinolytic activity produced by filamentous fungi associated with Antarctic marine sponges. *Biol. Res.* 51:28. doi: 10.1186/s40659-018-0177-4

Rosa, L. H., Pinto, O. H. B., Convey, P., Carvalho-Silva, M., Rosa, C. A., and Camara, P. E. A. S. (2020). DNA metabarcoding to assess the diversity of airborne fungi present over Keller Peninsula, King George Island, Antarctica. *Microb. Ecol.* doi: 10.1007/s00248-020-01627-1 [Online ahead of Print].

Rusman, Y., Held, B. W., Blanchette, R. A., He, Y., and Salomon, C. E. (2018). Cadopherone and colomitide polyketides from *Cadophora* wood-rot fungi associated with historic expedition huts in Antarctica. *Phytochemistry* 148:1.

Santos, J. A. D., Meyer, E., and Sette, L. D. (2020). Fungal community in antarctic soil along the retreating Collins Glacier (Fildes Peninsula, King George Island). *Microorganisms* 8:1145. doi: 10.3390/microorganisms8081145

Shi, L.-J., Wu, Y.-M., Yang, X.-Q., Xu, T.-T., Yang, S., Wang, X.-Y., et al. (2020). The cocultured *Nigrospora oryzae* and *Collectotrichum gloeosporioides*, *Irpex lacteus*, and the plant host *Dendrobium officinale* bidirectionally regulate the production of phytotoxins by anti-phytopathogenic metabolites. *J. Nat. Prod.* 83, 1374–1382. doi: 10.1021/acs.jnatprod.0c00036

Shi, T., Yu, Y.-Y., Dai, J.-J., Zhang, Y.-T., Hu, W.-P., Zheng, L., et al. (2021). New Polyketides from the Antarctic Fungus Pseudogymnoascus sp. HSX2#-11. *Mar. Drugs* 19:168.

Skehan, P., Storeng, R., Scudiero, D., Monks, A., Mcmahon, J., Vistica, D., et al. (1990). New colorimetric cytotoxicity assay for anticancer-drug screening. *J. Natl. Cancer Inst.* 82:1107.

Sun, C.-T., Wang, J.-P., Shu, Y., Cai, X.-Y., Hu, J.-T., Zhang, S.-Q., et al. (2020). A new tremulane sesquiterpene from *Irpex lacteus* by solid-state fermentation. *Nat. Prod. Res.* 1–6. doi: 10.1080/14786419.2020.1806272 [Online ahead of print].

Sun, C., Zhang, Z., Ren, Z., Yu, L., and Zhu, T. (2020). Antibacterial cyclic tripeptides from Antarctica-sponge-derived fungus *Aspergillus insulicola* HDN151418. *Mar. Drugs* 18:532.

Tagawa, M., Tamaki, H., Manome, A., Koyama, O., and Kamagata, Y. (2010). Isolation and characterization of antagonistic fungi against potato scab pathogens from potato field soils. *FEMS Microbiol. Lett.* 305, 136–142. doi: 10.1111/j.1574-6968.2010.01928.x

Wang, F., Ma, H., Hu, Z., Jiang, J., Zhu, H., Cheng, L., et al. (2017). Secondary metabolites from *Colletotrichum capsici*, an endophytic fungus derived from *Siegesbeckia pubescens* Makino. *Nat. Prod. Res.* 31, 1849–1854. doi: 10.1080/14786419.2016.1261346

Wang, M., Du, J.-X., Yang, H.-X., Dai, Q., Liu, Y.-P., He, J., et al. (2020). Sesquiterpenoids from cultures of the basidiomycetes *Irpex lacteus*. *J. Nat. Prod.* 83, 1524–1531. doi: 10.1021/acs.jnatprod.9b01177

Weng, Y., Lu, J., Xiang, L., Matsuura, A., Zhang, Y., Huang, Q., et al. (2011). Ganodermasides C and D, two new anti-aging ergosterols from spores of the medicinal mushroom *Ganoderma lucidum*. *Biosci. Biotechnol. Biochem.* 75, 800–803. doi: 10.1271/bbb.100918

Weng, Y., Xiang, L., Matsuura, A., Zhang, Y., Huang, Q., and Qi, J. (2010). Ganodermasides A and B, two novel anti-aging ergosterols from spores of a medicinal mushroom *Ganoderma lucidum* on yeast via UTH1 gene. *Bioorg. Med. Chem.* 18, 999–1002. doi: 10.1016/j.bmc.2009.12.070

Wu, G. (2016). Pharmaceutical composition of citicoline sodium and medicinal application thereof. China Patent No. 105753681A, Jul 13, Jiangsu, China.

Wu, P.-F., Ding, R., Tan, R., Liu, J., Hu, E.-M., Li, C.-Y., et al. (2020). Sesquiterpenes from cultures of the fungus *Phellinus igniarius* and their cytotoxicities. *Fitoterapia* 140:104415. doi: 10.1016/j.fitote.2019.104415

Wu, X., Lin, S., Zhu, C., Yue, Z., Yu, Y., Zhao, F., et al. (2010). Homo- and heptanor-sterols and tremulane sesquiterpenes from cultures of *Phellinus igniarius*. *J. Nat. Prod.* 73, 1294–1300.

Wu, Y.-M., Zhou, Q.-Y., Yang, X.-Q., Luo, Y.-J., Qian, J.-J., Liu, S.-X., et al. (2019). Induction of antiphytopathogenic metabolite and squalene production and phytotoxin elimination by adjustment of the mode of fermentation in cocultures of phytopathogenic *Nigrospora oryzae* and *Irpex lacteus*. *J. Agric. Food Chem.* 67, 11877–11882. doi: 10.1021/acs.jafc.9b04209

Xia, Q., Rufty, T., and Shi, W. (2021). Predominant microbial colonizers in the root endosphere and rhizosphere of turfgrass systems: *Pseudomonas veronii*, *Janthinobacterium lividum*, and *Pseudogymnoascus* spp. *Front. Microbiol.* 12:643904. doi: 10.3389/fmicb.2021.643904

Ying, Y. M., Shan, W. G., Zhang, L. W., and Zhan, Z. J. (2013). Ceriponols A–K, tremulane sesquitepenes from *Ceriporia lacerate* HS-ZJUT-C13A, a fungal endophyte of *Huperzia serrata*. *Phytochemistry* 95, 360–367.

Yu, G., Sun, Z., Peng, J., Zhu, M., Che, Q., Zhang, G., et al. (2019). Secondary metabolites produced by combined culture of *Penicillium crustosum* and a *Xylaria* sp. *J. Nat. Prod.* 82, 2013–2017.

Zhou, Q.-Y., Yang, X.-Q., Zhang, Z.-X., Wang, B.-Y., Hu, M., Yang, Y.-B., et al. (2018). New azaphilones and tremulane sesquiterpene from endophytic *Nigrospora oryzae* cocultured with *Irpex lacteus*. *Fitoterapia* 130, 26–30. doi: 10.1016/j.fitote.2018.07.018

Zhou, Z.-Y., Tang, J.-G., Wang, F., Dong, Z.-J., and Liu, J.-K. (2008). Sesquiterpenes and aliphatic diketones from cultures of the basidiomycete *Conocybe siliginea*. *J. Nat. Prod.* 71, 1423–1426. doi: 10.1021/np8002657